

DOI: 10.1002/ange.200600329

A Priori Theoretical Prediction of Selectivity in Asymmetric Catalysis: Design of Chiral Catalysts by Using Quantum Molecular Interaction Fields**

James C. Ianni, Venkatachalam Annamalai, Puay-Wah Phuan, Manoranjan Panda, and
Marisa C. Kozlowski*

Much effort has been devoted toward the development of asymmetric catalysts for the synthesis of chiral compounds in pure form.^[1] Despite this body of work, the science of asymmetric catalysis remains far from exact, and the process of finding a new catalyst usually requires a large investment of manpower and funding. Therefore, a major goal is the development of more efficient methods for identifying highly selective asymmetric catalysts. In terms of computational methods, the calculation of ground state and transition state energies^[2] for metal catalysts is promising.^[3] Even so, a detailed knowledge of the reaction mechanism is needed, and many variables must be evaluated requiring extensive time, effort, and resources. This communication illustrates the first example of rapid quantitative structure–selectivity relationship (QSSR) calculations being used to predict the enantioselectivities of new chiral catalysts. Subsequent synthesis and assessment of the new chiral catalysts in the asymmetric addition of Et₂Zn to benzaldehyde (Scheme 1) revealed that the QSSR calculations forecast the experimental results with a high degree of fidelity.

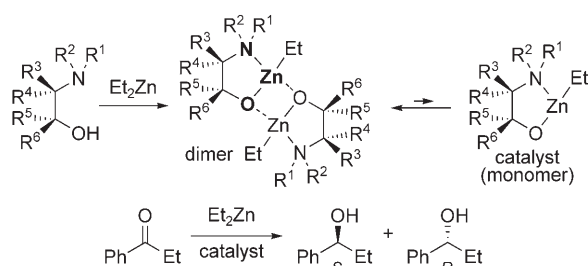
In a prior report^[4] we determined that grid-based QSSR methods^[5] derived from quantum mechanical molecular interaction fields can be used to generate statistically valid models that correlate enantioselectivities in the addition of Et₂Zn to PhCHO with catalyst geometries obtained from transition structures. The true test of this method lies in predicting the selectivity of catalysts with ligands that have not been tested and for which the experimental results cannot be easily anticipated based on previous results. To this end, we designed **P1**, a cyclohexane with *trans* amino and hydroxy

[*] Dr. J. C. Ianni, V. Annamalai, Dr. P.-W. Phuan, Dr. M. Panda, Prof. M. C. Kozlowski
Roy and Diana Vagelos Laboratories
Department of Chemistry
University of Pennsylvania
Philadelphia, PA 19104-6323 (USA)
Fax: (+1) 215-573-7165
E-mail: marisa@sas.upenn.edu

[**] Financial support of this research was provided by the NIH (GM59945). Computing resources from the NCSA (CHE020059) and the NSF CRIF program (CHE0131132) are acknowledged. We thank Steve Dixon, Giorgio Lauri, and Prof. Kenneth Merz for assistance with the QM-QSAR program. We are grateful to Bill Nugent for supplying the unpublished data for **P3**.



Supporting information for this article is available on the WWW under <http://www.angewandte.org> or from the author.



Scheme 1. Generation of the catalyst and the β -aminoalkoxide-catalyzed addition of Et_2Zn to PhCHO .

groups (Figure 1). This type of ligand, with a chiral quaternary alcohol carbon, is not found in the parameterization set **T1–T18** used to calibrate the QSSR model.^[6] Since syntheses of

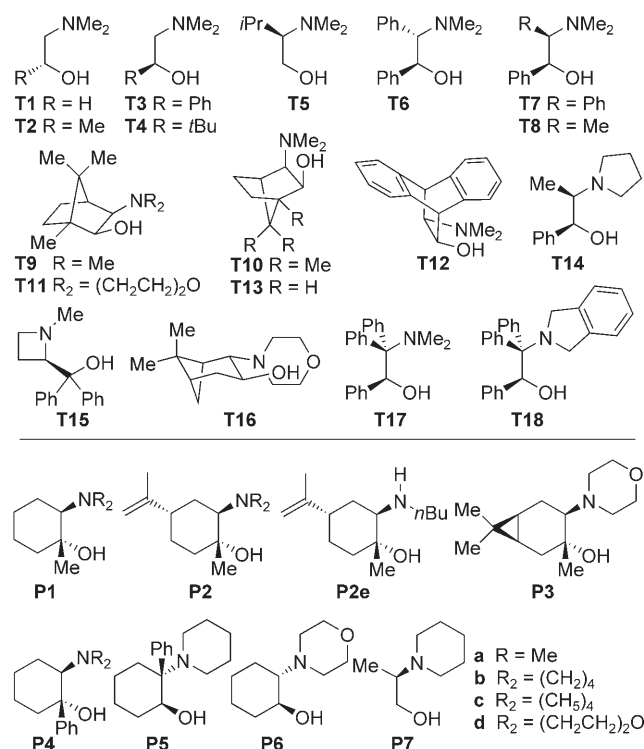


Figure 1. β -Amino alcohols used in parameterization (**T1–T18**) and a priori predictions (**P1–P7**).

P2^[7] and **P3**^[8] had been reported, we wished to predict the selectivities of **P1–P6**. When the QSSR model based on transition state structures^[4] was used to generate predictions, the standard deviations were high and the predictions were found to be dependent on the parameterization set. To solve these problems, further investigation of the QSSR protocol was undertaken.

It is highly desirable to be able to apply a QSSR protocol^[5] without knowing the reaction pathway (i.e., the transition state structures previously used in the parameterization).^[4] We have achieved this here using the catalyst geometries found in the ground state dimers (aligned by N, Zn, O atoms; bold in Scheme 1) of **T1–T18**.^[6] The geometry around the zinc atom is

critical as good QSSR models could not be obtained for the monomers (trigonal at Zn). The dimers (tetrahedral at Zn) likely reflect the interactions encountered during reaction (tetrahedral at Zn). The *syn* zinc dimers were selected as they have been identified crystallographically^[9] and in solution^[10] for the chiral catalysts.^[11] The geometry for the half of the calculated dimer of **T9** (PM3) was quite similar to the reported crystallographic structure (rmsd = 0.23 Å) as well as to other calculated dimers.^[10,12] Similarly, the geometry of the half dimer of **T9** matches closely with that portion in calculated transition states.^[13]

Use of the QSSR method with these dimers (aligned by N, Zn, O atoms; bold in Scheme 1) provided models that were highly accurate. Notably, these ground state structures were obtained much more readily and with less computational time than the corresponding transition structures. A “leave-two-out” analysis using all 153 combinations of 16 parameterization- and 2 prediction-set elements from **T1–T18** indicated a high degree of cross-validation for these internal predictions ($r_{\text{cv}}^2 = 0.85$, see the Supporting Information). Figure 2 illus-

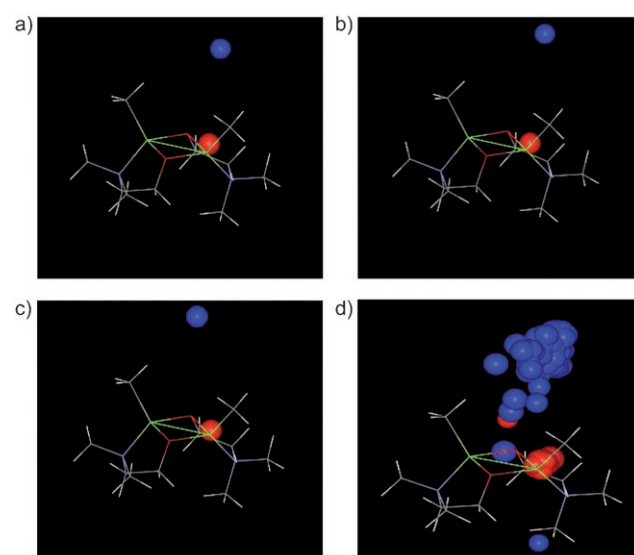


Figure 2. a–c) Several of the models from the “leave-two-out” analyses. d) Superimposed models from all 153 trials. Blue: *ee* value increases with increasing grid-point energy; red: *ee* value decreases.

trates the grid points (sphere centers) correlated to selectivity for three of the models from this analysis as well as an overlay of all 153 models. The method is robust as the models are relatively unaffected by the constitution of the parameterization set. In addition, these points indicate which portions of the catalyst are most important to the stereoselectivity. For example, the dimethylmethylene bridge of **T9** and **T11** correlates to high selectivity, whereas the phenyl group nearest the hydroxy group in **T6–T8** correlates to moderate selectivity.

With this model in hand, we generated predictions for catalysts derived from ligands **P1–P6**. In the first analysis (Table 1, single run) with the parameterization set comprising **T1–T18**, predicted ΔG values were obtained and translated into enantioselectivity values at 0°C (273 K). In a second

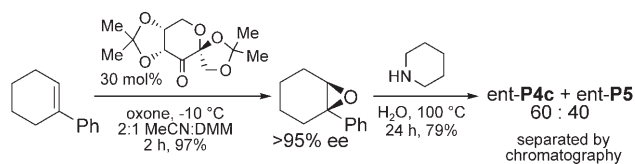
Table 1: QSSR a priori predictions for catalysts derived from **P1**–**P7**.

Ligand	Single run ^[a]		“Leave-two-out” ^[b]			CI % ee ^[e]	Expt. % ee ^[f]
	$\Delta G^{[c]}$	% ee ^[d]	Mean $\Delta G^{[c]}$	SD $\Delta G^{[c]}$	% ee ^[d]		
P1a	1.74	92.3	1.68	0.22	91.5	3.2	–
P1b	0.81	63.5	0.91	0.33	68.8	15.9	–
P1c	1.16	78.9	1.45	0.38	87.2	8.2	89
P1d	0.80	63.0	1.01	0.28	73.2	11.8	83
P2a	1.01	73.1	1.05	0.26	74.9	10.3	67
P2b	0.92	69.3	1.03	0.35	73.9	14.6	70
P2c	1.14	78.5	1.19	0.31	80.2	10.0	87
P2d	1.00	72.7	1.13	0.24	78.0	8.7	81
P2e	0.74	59.2	0.82	0.43	64.1	23.1	48
P3	1.11	77.4	1.26	0.29	82.3	8.4	84
P4a	2.88	99.0	2.68	0.31	98.6	0.8	–
P4b	2.10	96.0	2.01	0.38	95.2	3.2	–
P4c	3.61	99.7	3.77	0.77	99.8	0.3	97
P4d	3.67	99.8	3.78	0.75	99.8	0.2	94
P5	2.71	98.7	2.69	0.16	98.6	0.4	98
P6	0.89	67.6	0.93	0.21	69.8	9.8	59
P7	0.47	41.2	0.55	0.24	50.1	8.0	33

[a] Compounds **T1**–**T18** served as the parameterization set. [b] “Leave-two-out” cross-validating analysis using 16 compounds from **T1**–**T18** as the parameterization set (all 153 combinations). [c] Calculated ΔG in kcal mol^{−1}. [d] Generated from ΔG at 273 K; *S* enantiomer product. [e] 95 % confidence interval. [f] From reactions performed at 273 K. *S* enantiomer product.

analysis (Table 1, “leave-two-out”) all combinations of 16 parameterization-set elements from **T1**–**T18** were employed, resulting in 153 different models and 153 sets of predicted ΔG values for catalysts derived from **P1**–**P6**. From these data, 95 % confidence intervals for the predicted mean *ee* values were generated.

After these predictions were made, we discovered that Singaram et al. had reported the selectivities for catalysts derived from the limonene derivatives **P2**.^[14] We were delighted to find a high degree of correlation between the calculated and reported selectivities. The correlation was good even with the conformationally flexible *n*-butyl compound **P2e**. For **P3**, Nugent provided us with unpublished results (84 % *ee*) which agreed very well with the QSSR predictions (single 77 % *ee*, mean 82 % *ee*).^[15] To complete our study we synthesized representative examples of the remaining compounds in pure form using the protocol outlined in Scheme 2 for **P4c** and **P5**.^[16] We were excited to find that the experimental values for catalysts derived from **P1c**, **P1d**, **P4c**, **P4d**, **P5**, and **P6** (89, 83, 97, 94, 98, 59 % *ee*) were in good accord with our predictions (87, 73, 99, 99, 99, 69 % *ee*, respectively)^[17] and generally fell within the calculated 95 % confidence intervals. Notably, in accord with the calculations, a change from a methyl group (**P1**) to a phenyl group (**P4**) at C1 immediately next to the hydroxy group



Scheme 2. Synthesis of prediction-set β -amino alcohols **P4c** and **P5**. DMM = dimethoxymethane.

resulted in a dramatic improvement in enantioselectivity largely independent of the substituents on the nitrogen atom. Also in agreement with the calculations, the isopropenyl (**P2**) and cyclopropyl (**P3**) substitution was found to have little effect on the enantioselectivity (cf. **P1d**, **P2d**, **P3**).

To illustrate that the model provides good predictions for poorly selective as well as moderately and highly selective catalysts, further catalysts were screened computationally. Of those, **P7** was predicted to provide low selectivity (50 % *ee*) which was borne out in subsequent experiments (33 % *ee*). Overall, the agreement between the experimental values and the predictions for a variety of ligands was very good as illustrated in Figure 3 ($r^2_{\text{pred.}} = 0.87$). Based upon these results, the mixture of **P4c** and **P5** obtained during the ligand synthesis (Scheme 2) was also tested and provided the product with very high selectivity (97 % *ee*) as predicted by the model. Thus,

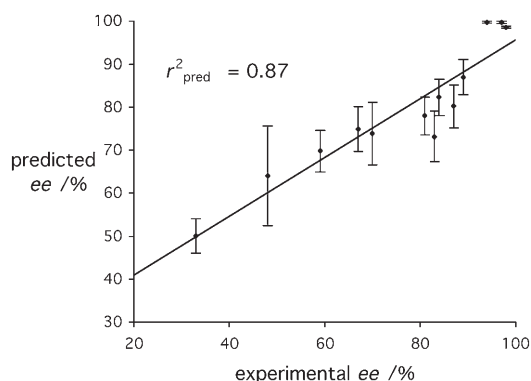


Figure 3. Plot of predicted vs. experimental enantiomeric excesses for catalysts derived from **P1**–**P7**.

the quantum QSSR model guided our discovery of this highly enantioselective catalyst system, which can be prepared in two simple steps from commercial materials.

Since the initial pioneering theoretical analyses (MP2/6-31G*/Zn//RHF/3-21G/Zn^[12] and B3LYP/6-31G*/Zn//RHF/3-21G/Zn^[13]) by Yamakawa and Noyori of the asymmetric alkylation of aldehydes, many groups have used various types of transition state calculations employing parameterized force fields (Q2MM^[3c]), semiempirical approaches (AM1,^[3a] PM3^[18]), mixed methods (RHF/LanL2DZ:UFF,^[19] RHF/LanL2DZ:MM3^[20]), DFT,^[21] and post-HF methods (MP2^[3b]) to understand or design selective chiral catalysts. Notably, the complexity of the system, the number of relevant structures, and the presence of the zinc atom require considerable computational resources for full ab initio or DFT calculations. For a set of nine catalysts, PM3 performed very well^[18] ($r^2_{\text{pred.}} = 0.85$) but was less satisfactory with a more diverse set of catalysts.^[19a] Other cases with multiple catalysts that per-

formed well utilized QM/MM methods^[19] ($r_{\text{pred.}}^2 = 0.43$) and single-point DFT calculations^[21] ($r_{\text{pred.}}^2 = 0.58$). Overall, these calculations were very good in their relative ranking of catalysts and for key transition structure features. The QSSR method identified substituents on the nitrogen atom and on the carbon atom adjacent to the hydroxy group as important to enantioinduction, in agreement with these transition state calculations. In addition, the QSSR method is able to identify other locations at which substitution is advantageous, for example, the distal bridging elements in **T9–T13** and the phenyl group in **P5**. Overall, our QSSR method performs as well as or better ($r_{\text{pred.}}^2 = 0.87$) than other methods, while requiring fewer computational resources since ground states are employed exclusively.

In conclusion, we have shown that grid-based QSSR methods can be used to predict catalyst enantioselectivities with a high degree of accuracy and precision. This method requires knowledge of only the ground state catalyst structure. The empirical models are easily assembled from a small set of ligands and their experimentally measured selectivities such as might be determined in preliminary screening. Relatively quick theoretical calculations provide models that allow a researcher to readily distinguish poorly, moderately, and highly selective catalysts. Within a catalyst series, modifications that result in relatively small changes (i.e., **P2a–P2e**) can also be estimated with a good degree of reliability. Studies are underway using this computational method with other reactions, and preliminary results are promising.^[22] In addition, the readily prepared catalysts (two steps) that we have discovered are being explored in other transformations.

Received: January 25, 2006

Keywords: asymmetric addition · benzaldehyde · enantioselectivity · structure–activity relationships · zinc

- [1] *Comprehensive Asymmetric Catalysis* (Eds.: E. N. Jacobsen, A. Pfaltz, H. Yamamoto), Springer, New York, **1999**.
- [2] a) ACS Symposium Series 721: *Transition State Modeling for Catalysis* (Eds.: D. G. Truhlar, K. Morokuma), American Chemical Society, Washington, DC, **1999**; b) S. Niu, M. B. Hall, *Chem. Rev.* **2000**, *100*, 353–406.
- [3] For the reaction in Scheme 1: designing catalysts using transition state (TS) calculations: a) frozen TS core: A. Vidal-Ferran, A. Moyano, M. A. Pericás, A. Riera, *Tetrahedron Lett.* **1997**, *38*, 8773–8776; b) MP2/LanL2DZ//HF/LanL2DZ: M. C. Kozłowski, M. Panda, *J. Org. Chem.* **2003**, *68*, 2061–2076. For comments on the complexity of the transition state calculations: c) T. Rasmussen, P.-O. Norrby, *J. Am. Chem. Soc.* **2003**, *125*, 5130–5138.
- [4] M. C. Kozłowski, S. Dixon, M. Panda, G. Lauri, *J. Am. Chem. Soc.* **2003**, *125*, 6614–6615.
- [5] For other QSAR applications in enantioselective catalysis see: a) J. D. Oslob, B. Åkermar, P. Helquist, P. O. Norrby, *Organometallics* **1997**, *16*, 3015–3021; b) K. B. Lipkowitz, M. J. Pradhan, *J. Org. Chem.* **2003**, *68*, 4648–4656; c) S. Alvarez, S. Schefzick, K. Lipkowitz, D. Avnir, *Chem. Eur. J.* **2003**, *9*, 5832–5837; d) M. Hoogenraad, G. M. Klaus, N. Elders, S. M. Hooijschuur, B. McKay, A. A. Smith, E. W. Damen, *Tetrahedron: Asymmetry* **2004**, *15*, 519–523; e) J. B. van der Linden, E. J. Ras, S. M. Hooijschuur, G. M. Klaus, N. T. Luchters, P. Dani, G. Verspui, A. A. Smith, E. W. P. Damen, B. McKay, M. Hoogenraad, *QSAR Comb. Sci.* **2005**, *24*, 94–98; f) S. Sciabola, A. Alex, P. D. Higginson, J. C. Mitchell, M. J. Snowden, I. Morao, *J. Org. Chem.* **2005**, *70*, 9025–9027.
- [6] Experimental selectivities for **T1–T18**: a) M. Kitamura, S. Suga, K. Kawai, R. Noyori, *J. Am. Chem. Soc.* **1986**, *108*, 6071–6072; b) L. Pu, H.-B. Yu, *Chem. Rev.* **2001**, *101*, 757, and references therein.
- [7] C. T. Goralski, B. Singaram, W. Chrisman, US Patent 6362373B1, **2002**.
- [8] a) G. S. Kauffman, G. D. Harris, R. L. Dorow, B. R. P. Stone, R. L. Parsons, Jr., J. A. Pesti, N. A. Magnus, J. M. Fortunak, P. N. Confalone, W. A. Nugent, *Org. Lett.* **2000**, *2*, 3119–3121; b) R. L. Parsons, J. M. Fortunak, R. L. Dorow, G. D. Harris, G. S. Kauffman, W. A. Nugent, M. D. Winemiller, T. F. Briggs, B. Xiang, D. B. Collum, *J. Am. Chem. Soc.* **2001**, *123*, 9135–9143.
- [9] M. Kitamura, S. Okada, S. Suga, R. Noyori, *J. Am. Chem. Soc.* **1989**, *111*, 4028–4036.
- [10] M. Kitamura, M. Yamakawa, H. Oka, S. Suga, R. Noyori, *Chem. Eur. J.* **1996**, *2*, 1173–1181.
- [11] With homochiral catalysts, *syn* dimers have been observed experimentally: a) E. Hecht, *Z. Anorg. Allg. Chem.* **2000**, *626*, 2223–2227; b) K. Nakano, K. Nozaki, T. Hiyama, *J. Am. Chem. Soc.* **2003**, *125*, 5501–5510. With achiral catalysts, *anti* dimers predominate: c) M. R. P. van Vliet, J. T. B. H. Jastrzebski, G. van Koten, K. Vrieze, A. L. Spek, *J. Organomet. Chem.* **1983**, *251*, C17–C21; d) M. R. P. van Vliet, G. van Koten, P. Buysingh, J. T. B. H. Jastrzebski, A. L. Spek, *Organometallics* **1987**, *6*, 537–546; e) J. T. B. H. Jastrzebski, J. Boersma, G. van Koten, W. J. J. Smeets, A. L. Spek, *Recl. Trav. Chim. Pays-Bas* **1988**, *107*, 263–266; f) M. Kitamura, S. Suga, M. Niwa, R. Noyori, *J. Am. Chem. Soc.* **1995**, *117*, 4832–4842.
- [12] M. Yamakawa, R. Noyori, *J. Am. Chem. Soc.* **1995**, *117*, 6327–6335.
- [13] M. Yamakawa, R. Noyori, *Organometallics* **1999**, *18*, 128–133.
- [14] D. Steiner, S. G. Sethofer, C. T. Goralski, B. Singaram, *Tetrahedron: Asymmetry* **2002**, *13*, 1477–1483.
- [15] a) W. A. Nugent, personal communication; b) Subsequent to our calculations a report of 81% *ee* for **P3** in this same reaction appeared: S. N. Joshi, S. V. Malhotra, *Tetrahedron: Asymmetry* **2003**, *14*, 1763–1766.
- [16] See the Supporting Information for further details and full characterization. Epoxidation was accomplished with Shi's protocol (Z. Wang, Y. Tu, M. Frohn, J. Zhang, Y. Shi, *J. Am. Chem. Soc.* **1997**, *119*, 11224–11235) and epoxide opening with Singaram's conditions (see reference [14]).
- [17] The enantiomers of the predicted catalysts **P1**, **P4**, and **P5** were synthesized and yielded the enantiomer (*R*) opposite to that predicted (*S*).
- [18] B. Goldfuss, K. N. Houk, *J. Org. Chem.* **1998**, *63*, 8998–9006; C. Jimeno, M. Pastó, A. Riera, M. A. Pericás, *J. Org. Chem.* **2003**, *68*, 3130–3138.
- [19] a) B. Goldfuss, M. Steigelmann, S. I. Khan, K. N. Houk, *J. Org. Chem.* **2000**, *65*, 77–82; b) B. Goldfuss, M. Steigelmann, F. Rominger, *Eur. J. Org. Chem.* **2000**, 1785–1792.
- [20] J. Vázquez, M. A. Pericás, F. Maseras, A. Lledós, *J. Org. Chem.* **2000**, *65*, 7303–7309.
- [21] DFT BP86/DN**//PM3 M. Sosa-Rivadeneira, A. Muñoz-Muñoz, C. Anaya de Parrodi, L. Quintero, E. Juaristi, *J. Org. Chem.* **2003**, *68*, 2369–2375.
- [22] P.-W. Phuan, J. C. Ianni, M. C. Kozłowski, *J. Am. Chem. Soc.* **2004**, *126*, 15473–15479.